Giaouris D, Papadopoulos A, Seferlis P, Voutetakis S, Papadopoulou S.

Power grand composite curves shaping for adaptive energy management of hybrid microgrids.

***Renewable Energy* 2016, 95, 433-448.**

Power Grand Composite Curves Shaping For Adaptive Energy Management of Hybrid Microgrids

Damian Giaouris[1,4]; Athanasios I. Papadopoulos[1*]; Panos Seferlis[1,3] ;Spyros Voutetakis[1]; Simira Papadopoulou[1,2]

[1]Chemical Process and Energy Resources Institute,

Centre for Research and Technology Hellas, Thermi-Thessaloniki, Greece

[2]Department of Automation Engineering, Alexander Technological Educational Institute of Thessaloniki, Thessaloniki, Greece

[3]Aristotle University of Thessaloniki, Department of Mechanical Engineering,

Thessaloniki, Greece

[4] Newcastle University, School of Electrical and Electronic Engineering,

Newcastle upon Tyne, UK

[*] Corresponding author: spapadopoulos@cperi.certh.gr

Abstract:

This work proposes a systematic approach for the adaptive identification and implementation of efficient power management strategies (PMS) in the course of operation of hybrid renewable energy microgrids. The approach is based on the temporal evolution of the system power grand composite curve (PGCC), which is adaptively shaped within short-term time intervals to form a sequence of decisions that indicate the instant and duration of activation of different subsystems, thereby offering efficient utilization of resources and equipment to meet specific targets. It builds on from previous work done by the authors, where PGCC were used to identify the optimum PMS from an existing set of PMSs. More specifically, it involves a stored energy targeting step that exploits the PGCC to identify the desired operational profile of an accumulator during a prediction horizon in order to avoid the violation of constraints and satisfy the system operating goals. The identified energy targets are subsequently enforced through a sequence of control actions that enable the exact matching of the desired PGCC hence representing the selected PMS. The proposed method is elaborated graphically for multiple potential system operating goals and is supported by a formal mathematical model that captures system structural and temporal characteristics. It is further implemented on an actual hybrid microgrid considering multiple RES-based energy generation and storage options.

Keywords: Energy Management, Power Pinch Analysis, Grand Composite Curves, Hybrid Renewable Energy Systems, Process Integration

Nomenclature

BAT	Battery
BF	Low pressure (buffer) storage tanks
C_l	Capacity of accumulator *l*
CMP	Compressor
DSL	Diesel generator
EL	Electrolyzer
$F^{j}_{m \to n}(t)$	State of the flow *j* between the nodes *m* and *n*
FC	Fuel cell
FT	Long-term storage tank

H	Overall time span
H2HP	Hydrogen in high pressure
H2LP	Hydrogen in low pressure
H2O	Water
L	Logical operator
LD	Load
$Lo_i^{SOAcc^l}$	Lower desired limit for accumulator *l*
$MOES$	Maximum outsourced energy supply
N_c	Number of steps in control horizon
N_p	Number of steps in prediction horizon
OES	Outsourced energy supply
P_i^j	Amount of energy or mater per time unit of the flow *j* that may be produced or consumed by a converter *i*
PGCC	Power Grant Composite Curve
PMS	Power Management Strategy
POW	Electrical power
PV	Photovoltaic panels
Q	Set of all available PMS
RES	Renewable Energy Sources
Rs	Set of resources
$SOAcc^l$	State of accumulator *l*
T	End of time interval
t_{Lo}	Instant when $SOAcc^l$ reaches the value of the limit *Lo*
t_{min}	Instant when $SOAcc^l$ reaches the minimum value of $SOAcc^{l,q_k}$ in interval *k*
t_0	Beginning of time interval under study
$Up_i^{SOAcc^l}$	Upper operating limit for accumulator *l*
WG	Wind generator
WT	Water tank

Greek Symbols

ΔT	Duration of time interval
$\varepsilon_i(t)$	Binary variable that represents the state of converter *i*
$\rho_i^{SOAcc^l}$	Binary variable associated with temporal conditions in accumulator *l*

Subscripts/ Superscripts

Acc	Accumulator
Avl	Available
Conv	Converter
i	Index of converter or accumulator
Gen	General
j	Flow for a converter or accumulator
k	Time interval
l	Accumulators as part of the set of Resources
Mat	Materials
max	Maximum
min	Minimum

n, m	Resources (converters or accumulators) indicating the type of equipment employed to perform conversion and accumulation tasks $m, n \in Rs, m \neq n$
Nrg	Energy

39

1. Introduction

Micro grids based on renewable energy sources (RES) are receiving increased attention worldwide as they are required to support isolated and non-grid connected applications. To address the intermittent nature of largely unpredictable environmental phenomena, such systems transform RES into dependable energy flows by simultaneous utilisation of different types of conversion equipment and storage media (e.g. PV panels, wind generators, chemical energy accumulators, hydrogen and so forth). The resulting infrastructures combine multiple subsystems of heterogeneous characteristics that need to operate efficiently while satisfying power demands based entirely on RES. The complex synergies and interactions that emerge among such components raise the need for efficient decision making as potential operating alternatives unravel simultaneously with an increasing number of diverse components that become involved in the operations of the system. This decision making is generally addressed through power management strategies (PMS) (Giaouris et al., 2013) which represent a complex sequence of actions offering efficient utilization of resources and equipment to meet specific targets. Such actions account for decisions regarding the appropriate instant to activate/deactivate different subsystems, the duration of operation of a particular subsystem, the amount or type of energy carrier to use (e.g., electricity, hydrogen in high or low pressure, water) and so forth. They also depend on several criteria involving the availability of power from RES with respect to the demand (lack or excess), the availability of energy carriers in storage and the previous state of operation of different sub-systems (Ipaskis et al., 2008), to name but a few. Such diverse characteristics give rise to a large number of potential PMS. Efficient operation depends on the selection of the PMS that best satisfies the demands of the targeted application in view of RES variability, while maintaining a smooth system operation and protecting the individual components from malfunctions due to over- or under-utilization. This is clearly a non-trivial task requiring the use of systematic approaches to identify targets of efficient operation which can be subsequently interpreted as appropriately fitted operating realizations.

The recently proposed power Pinch concepts (grand composite curves (Bandyopadhyay 2011) and composite curves (Wan Alwi et al. 2012a)) represent one such approach, allowing the investigation of complex energy systems based on the identification of insights pointing towards optimum decisions. Such methods have been inspired from the well-known heat Pinch (Linhoff and Flower 1978) and evolved to sophisticated tools (Smith 2005) that allow for the analysis of complex energy systems (Varbanov et al. 2012). A major advantage of these methods is their implementation in the form of intuitive and easy to develop graphical interfaces (e.g., grand composite curves), whereas the underlying principles are often efficiently represented using rigorous mathematical tools (e.g., flexible process models combined with optimization algorithms). Regardless of the realization, Pinch methods allow the user to easily identify, review, and analyze potentially useful design and operating options (Klemeš and Varbanov 2013). A recent overview of Pinch analysis and mathematical programing for process integration is presented in Klemeš (2013).

Focusing on electrical systems, Pinch-based analysis methods utilize composite or grand composite curves similarly to the traditional heat Pinch; however, the associated sink and source streams are plotted in power versus time diagrams. In this context, a method proposing the identification of energy recovery targets using the grand composite curves (GCC) analysis approach was reported in Bandyopadhyay (2011) addressing the optimal sizing of power generation systems in the form of an optimization problem. Priya and Bandyopadhyay (2013) also proposed an approach for power systems planning considering a Pinch-based analysis for emissions targeting. Work presented in Wan Alwi et al. (2012a) proposed the power Pinch analysis (PoPA) method to determine the minimum electricity targets for systems comprising hybrid renewable energy sources. The graphical power Pinch analysis method takes the form of numerical tools in Mohammad Rozali et al. (2013a) such as the power cascade analysis (PoCA) and storage cascade table (SCT) in order to facilitate the precise allocation of power and electricity targets in power generation systems. Work presented in Mohammad Rozali et al. (2013b) extends the numerical power Pinch method by additionally

considering power losses during conversion, transferring, and storage including sizing considerations (Wan Alwi et al. 2012b). The method is applied in the optimization of a pumped hydro-storage system in Mohammad Rozali et al. (2013c) that is further extended in Mohammad Rozali et al. (2014a) to address the optimal sizing of hybrid power generation systems. Recent work presented in Wan Alwi et al. (2013) proposed the outsourced and storage electricity curves (OSEC) to visualize the required minimum outsourced electricity and the current storage capacity at each time interval during startup and operation of hybrid power systems. Methods for load shifting that may lead to further reductions of the maximum storage capacity and the maximum power demand in hybrid systems are also proposed in Mohammad Rozali et al. (2014b) using power Pinch analysis, whereas combined load shifting and design is proposed in Ho et al. (2013a). Work presented in Ho et al. (2013b) proposed the stand-alone hybrid system, power Pinch analysis method (SAHPPA), which is a graphical tool employing new ways of utilizing the demand and supply through composite curve methods. Recently, work presented in Ho et al. (2014) adapted the power Pinch concept in the electricity system cascade analysis (ESCA) approach to optimize distributed energy generation systems, while this approach was used for the optimum sizing and operation of a solar/wind/battery hybrid system (Zahboune et al. 2014). The PoPA method has also been transformed into the extended PoPA method (Esfahani et al. 2015) to address the design of hybrid systems with battery and hydrogen storage. Mohammad Rozali et al. (2015) proposed a power Pinch analysis tool called the AC/DC modified storage cascade to optimise the hybrid power generation systems by considering various storage technologies.

Recently, Giaouris et al. (2015) exploited the Power Grand Composite Curves (PGCC) approach (originally proposed in Bandyopadhyay 2011), focusing explicitly on the operation of hybrid renewable energy systems with different energy carriers and storage options under the influence of multiple different PMS. The authors showed that multiple Pinch points appear either simultaneously or at different instants when different energy carriers and operating goals are considered. Such

115 points may indicate the energy that needs to be recovered from RES or internal system resources in
116 order to avoid using outsourced electricity from non-RES, the energy that needs to be utilized to
117 avoid overcharging the different storage options and so forth. It was observed that the appearance
118 of multiple Pinch points often resulted in satisfaction of one operating goal at the expense of another
119 (e.g. avoidance of outsourced electricity from non-RES at the expense of battery overcharging).
120 This was addressed through the prioritization of the operating goals that are to be satisfied using the
121 most appropriate PMS from a pool of several alternatives. The selected PMS was the one that
122 resulted in the satisfaction of the primary operating goal and in the smallest possible violation of
123 other secondary goals during a given time interval. This idea was implemented within a framework
124 that exploited the PGCC method to perform two functions: a) the identification of renewable energy
125 recovery targets within a short term prediction horizon, and b) the temporal reallocation of the grid
126 subsystems within a control horizon based on selection of the PMS that best matches the identified
127 targets. The PGCC was therefore exploited for the first time within a model predictive control
128 framework aiming to satisfy the system operating goals. This idea was then tested compared to
129 utilizing a single PMS throughout the system operation and regardless of the available RES, as is
130 mostly the case in commissioned smart grids. The results from exploiting multiple PMS showed a
131 significant reduction in the usage of non-renewable external sources through the recovery of the
132 required energy from internal sources with simultaneous reduction in the utilization of delicate
133 equipment such as the fuel cell (hence reducing the associated wear and tear).
134 The concept of the PGCC proved very useful in terms of targeting the necessary energy needs. On
135 the other hand, the selection among pre-determined PMS is very useful for practical reasons as the
136 safety and operating limits may be well-tested prior to utilization, offering a predictable system
137 response. However, PMS are essentially pre-determined hierarchical decision structures based on
138 conditions imposed on a sequence of operating parameters that need to be evaluated prior to
139 deciding which sub-system will be activated or deactivated and with what duration (Giaouris et al.,

2015). A recent review of various PMS implementations on hybrid energy grids (Chauhan and Saini, 2014) and a more recent work also reviewing several of them (Bizon et al., 2015) indicate that to achieve high system performance it is important to vary both the sequence of evaluation of each parameter and the thresholds of the corresponding conditions. For example, Giaouris et al. (2015) developed 9 PMS where the decision structures are combinations of the availability of power from RES, the availability of energy stored in the battery or of hydrogen stored in the tanks and the length of the hysteresis zones (i.e., fixed throughout, variable depending on the time of year or on the duration of activation of each sub-system). Despite the larger number of employed PMS compared to the average of 3 PMS mostly considered in published literature (Chauhan and Saini, 2014), the obtained results indicated that it is necessary to pre-determine a very large number of PMS in order to ensure that no operating constraint is violated and that the energy targets identified from the PGCC may be fully matched and exploited. This is practically difficult because the sub-system interactions represented within a PMS become increasingly complex as more sub-systems are added, whereas the RES behaviour always remains unpredictable.

To address these challenges this work proposes a new approach which exploits the PGCC to determine the PMS that simultaneously matches all the identified energy targets in the course of the system operation. The specific operational goals are to address all the identified energy targets and at the same time minimise the requirement for external energy supply. In the proposed approach the desired PMS results from targeted alterations imposed on the system PGCC within a specified time horizon, hence avoiding the necessity for pre-determining various different PMS. Following the concepts of Pinch analysis, the PGCC is first shifted to determine the energy recovery targets and is then matched exactly by activating appropriate equipment at selected instants so that the violation of operating constraints is completely avoided. This results in a new overall shape of the initially shifted PGCC of the system which represents the new PMS. The proposed approach explores operating limits that represent different operating goals in the context of a model predictive

framework. It has to be noted here that even though this method can address the energy requirements set by the user, it does not explicitly take into account the cost of operation (for example the battery's wear). Having said that, it does take the overall cost implicitly into account from the operating limits set by the user.

2. System models and Pinch concept

2.1 Structural model of motivating system

The system that motivated this work has been constructed and commissioned on location in Greece (Ipsakis et al., 2009; Ziogou et al., 2011) and consists of a *LD* (local load that needs to be satisfied), *PV* (photovoltaic panels), a *BAT* (battery), a *FC* (fuel cell), an *EL*(electrolyser), a BF (buffer tank for hydrogen), a *CP* (compressor), a *FT* (final tank for hydrogen), a *WT* (water tank) and a *DSL* (diesel generator) which is used only as a back-up option. A conceptual flowsheet representing the system as a directed graph is shown in Figure 1. Regardless of the particular equipment types employed in the system of Figure 1, hybrid RES-based flowsheets may be represented through interconnected converters and accumulators that convert or store material and energy; flows and accumulation at different instants are the key features that drive their operation (Giaouris et al., 2013). The activation instance and operating period of each converter are important operating parameters as they determine their utilisation frequency. The state (level) of accumulated energy or materials in the form of diverse energy carriers is also important, prompting the activation of different converters based on their technical characteristics. The duration of activation further depends on a hysteresis based mode of operation, i.e. on whether the converter was active in the previous instant. The combination of these temporal characteristics form complex operating rule sequences called PMS which may be represented through generic models (Giaouris et al., 2013)

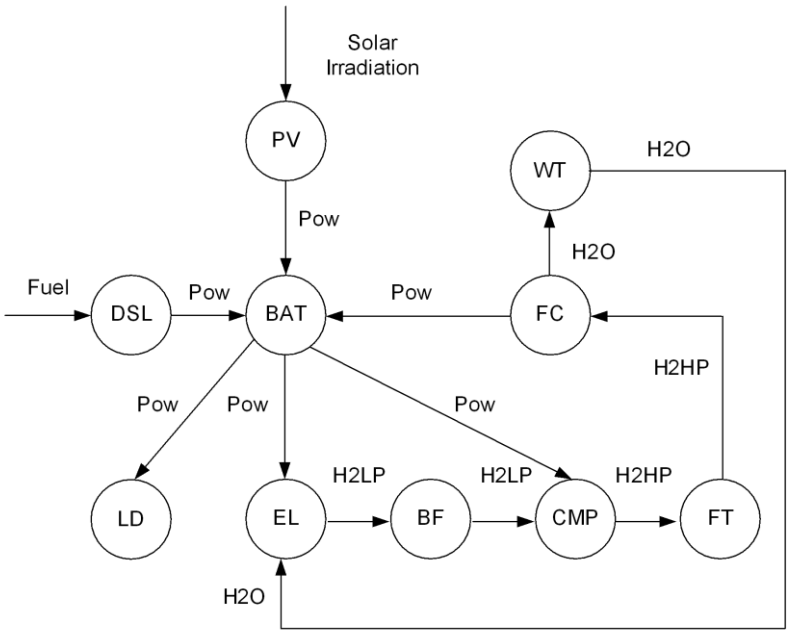

Figure 1: Conceptual representation of a typical hybrid microgrid with flows as a directed graph

In this generic context, each device is represented by a node and the edges between the nodes appear when the device is activated. The nodes are classified in two sets, the set of converters (Rs^{Conv}) and the set of accumulators (Rs^{Acc}). For the system considered in this work these sets contain the following components $Rs^{Acc} = \{BAT, FT, BF, WT\}$ and $Rs^{Conv} = \{PV, DSL, EL, FC, CMP\}$. The connection between two nodes is a flow of either energy (for example electrical in the connection *FC→BAT*) or matter (for example hydrogen in the connection *FT→FC*). The different types of flow define a set called *Flow* with $Flow = \{Pow, H2HP, H2LP, H2O\}$. In this set *Pow* is electrical power, *H2HP* is hydrogen at high pressure stored in the final tank, *H2LP* is hydrogen at low pressure stored in the buffer tank and *H2O* is water stored in the water tank. For this case study an edge is possible to exist only between an accumulator and a converter (and vice-versa), i.e. the connection between two different accumulators is not considered as it can be represented by another accumulator. Based on a similar concept as of that of dynamical systems (Kuznetsov, 2004) the state *S* of a graph (i.e. of the microgrid) is given by the states of the nodes and edges. These states are variables that fully describe the edges and the nodes, defined as follows:

- For the edges a state must describe its existence, and the type/amount of flow that it contains. This is represented by the variable $F^{j}_{m\to n}(t)$ with $j \in Flow$ and *m*, *n* two adjacent nodes. When the edge does not exist $F^{j}_{m\to n}(t)$ is zero.
- For accumulators the state is the normalized amount of stored matter or energy, represented by the variable $SOAcc^{l}(t) \in [0,1], l \in Rs^{Acc}$
- For the converters the state is their status (i.e. if they are activated or not) represented by the variable $\varepsilon_i(t) \in \{0,1\}, i \in Rs^{Conv}$

The state of the graph is therefore fully described as follows:

$$S = \left\{ F^{j}_{m\to n}(t), SOAcc^{l}(t), \varepsilon_i(t) \right\}, l \in Rs^{Acc}, i \in Rs^{Conv}, m,n \in Rs^{Acc} \times Rs^{Conv}, j \in Flow \quad (1)$$

Note that all these states are coupled together (as in typical dynamical systems) because the states of the edges ($F^{j}_{m\to n}(t)$) depend on the states of the converters ($\varepsilon_i(t)$), the states of the converters depend on the states of the accumulators ($SOAcc^{l}(t)$) and the states of the accumulators depend on the state of the edges ($F^{j}_{m\to n}(t)$)

2.2 Temporal model of motivating system

The next step required to fully describe the proposed model is to include the temporal evolution of the state vector *S*. For an accumulator *l* its state $SOAcc^{l}$ is effectively an integrator and it depends on its capacity C_l and the flows $F^{j}_{m\to n}(t)$ that are directed towards and away from the accumulator:

$$SOAcc^{l}(t) = SOAcc^{l}(t-1) + \frac{\sum_{k_1 \in Rs^{Conv}} F^{j}_{k_1\to l}(t) - \sum_{k_2 \in Rs^{Conv}} F^{j}_{l\to k_2}(t)}{C_l}, l \in Rs^{Acc}, j \in Flow \quad (2)$$

The state of an edge $F^{j}_{m\to n}(t)$ is defined as follows:

$$F^{j}_{m\to n}(t) = \varepsilon_i(t) \cdot P_i^{\,j}, i \in \{m,n\}, j \in Flow \quad (3)$$

where P_i^j is the amount of energy or matter per unit of time that may be converted by the i-th unit and ε_i is the state of the corresponding converter *i*. Variables P_i^j are used as decision parameters and their values are identified by the performed Pinch analysis which is elaborated in the subsequent sections. The Pinch analysis determines the resulting PMS through variable ε_i which depends on specific conditions regarding the availability or demand of material or energy in the accumulators. The variable value depends on the following three factors that obtain binary variables (Giaouris et al., 2013):

1. $\varepsilon_i^{Avl}(t)$ which represents the availability of material or energy that will be converted.
2. $\varepsilon_i^{Req}(t)$ which represents the demand for material or energy in a conversion.
3. $\varepsilon_i^{Gen}(t)$ which represent other potentially desired condition(s) that are not associated with the above.

The availability or demand for material or energy to perform a conversion depends on the state of the accumulators. This is quantified through a binary variable ρ that is 1 when there is availability or demand and 0 otherwise:

$$\varepsilon_i^{Avl}(t) = \underset{l \in Rs^{Acc}}{L^{Avl}}\left(\rho_i^{SOAcc^l}\right)$$
$$\varepsilon_i^{Req}(t) = \underset{l \in Rs^{Acc}}{L^{Req}}\left(\rho_i^{SOAcc^l}\right) \quad (4)$$

where L^{Avl} and L^{Req} are logical operators that are applied on the variables ρ which in turn quantify the requirement and the availability of/from the accumulator *l*. The general condition can depend on a node or an edge but in most cases it depends on the state of other converters and therefore it can be defined as follows:

$$\varepsilon_i^{Gen}(t) = \underset{i_c \in Rs^{Conv}}{L^{Gen}}\left(\rho_i^{i_c}\right) \quad (5)$$

where again L^{Gen} is a logical operator. The above are combined into variable ε using a logical operator L:

$$\varepsilon_i(t) = L\left(\varepsilon_i^{Avl}(t), \varepsilon_i^{Req}(t), \varepsilon_i^{Gen}(t)\right) \quad (6)$$

To define the variables $\rho_i^{SOAcc^l}(t)$ we use relational operators applied on the state of various accumulators and predefined variables set again by the PMS. For example see the following expression:

$$\rho_i^{SOAcc^l}(t) = \left\lceil SOAcc^l(t) < Lo_i^{SOAcc^l}(t) \right\rceil \quad (7)$$

It implies that the variable $\rho_i^{SOAcc^l}(t)$ will be 1 if the state of the accumulator l is less than the variable $Lo_i^{SOAcc^l}$. This is a lower (*Lo*) limit in the energy or material available in the accumulator which determines when a converter will be activated. A similar expression may apply for upper limits (*Up*). It has to be mentioned here that in practical applications a hysteresis zone is also used to avoid chattering problems (Giaouris et al., 2013). In our current work we will generate an additional, general structure of conditions that affect the value of the ρ variables which are independent from the state of the accumulators and enable the derivation of the desired PMS using a Pinch analysis approach based on the PGCC concept.

2.3 Example of structural and temporal modelling

In order to elaborate how equations (3)-(7) support the development of a PMS, consider two nodes from the aforementioned energy system, the *FC* and the *BAT*. The *FC* is fed with *H2HP* by the *FT* and produces *H2O* (delivered to the *WT*) and *Pow* which is given to the battery. The adjacent edges of the *FC* include the edge that connects it to the *FT* (the flow is *H2HP*), to the *WT* (the flow is *H2O*) and to the battery (the flow is *Pow*); these edges will appear/exist when the *FC* is activated. The state of the *FC* (i.e. the instant of activation) depends on several conditions which determine

the overall PMS. These conditions may be expressed through the variable ρ. The FC can therefore be activated when:

1. There is demand for *Pow* because the *BAT* is not adequately charged, i.e. the $SOAcc^{BAT}$ is less than a predefined value $Lo_{FC}^{SOAcc^{BAT}}(t)$:

$$\rho_{FC}^{SOAcc^{BAT}}(t) = SOAcc^{BAT}(t) < Lo_{FC}^{SOAcc^{BAT}}(t) \quad (8)$$

2. There is availability of hydrogen because the *FT* is not empty, i.e. the $SOAc^{FT}$ is more than a predefined value $Lo_{FC}^{SOAcc^{FT}}$:

$$\rho_{FC}^{SOAcc^{FT}}(t) = SOAcc^{FT}(t) > Lo_{FC}^{SOAcc^{FT}} \quad (9)$$

3. There is available space in the *WT* because it is not full, i.e. the $SOAcc^{WT}$ is less than a predefined value $Up_{FC}^{SOAcc^{WT}}$:

$$\rho_{FC}^{SOAcc^{WT}}(t) = SOAcc^{WT}(t) < Up_{FC}^{SOAcc^{WT}}(t) \quad (10)$$

4. The DSL remains inactive as it was in the previous instant (t-1), i.e. there is no reason to activate it if we can use RES to generate the necessary *Pow*:

$$\varepsilon_{DSL}(t-1) = 0 \quad (11)$$

The above conditions assume an ON-OFF behaviour without hysteresis. More details regarding the use of a hysteresis zone can be found in Giaouris et al. (2013). Conditions (9) and (10) refer to availability and condition (8) refers to demand hence the corresponding superscripts '*Avl*' and '*Req*' need to be used for the ε variables. Condition (11) is a general one which refers to the relation of the *FC* with another converter (*DSL*) hence the *Gen* superscript needs to be used. Using the appropriate logical operators L in equations (4)-(6) the equations for the ε variables take the following form:

$$\varepsilon_{FC}^{Avl}(t) = \rho_{FC}^{SOAcc^{FT}}(t) \wedge \rho_{FC}^{SOAcc^{WT}}(t)$$
$$\varepsilon_{FC}^{Req}(t) = \rho_{FC}^{SOAcc^{BAT}}(t)$$
$$\varepsilon_{FC}^{Gen}(t) = \left[\varepsilon_{DSL}(t^{-}) = 0\right] \quad (12)$$
$$\varepsilon_{FC}(t) = \varepsilon_{FC}^{Avl}(t) \wedge \varepsilon_{FC}^{Req}(t) \wedge \varepsilon_{FC}^{Gen}(t)$$

Equations (7)-(12) represent the mathematical expression of the selected PMS and may now be used to calculate the necessary flows around the *FC*. For example, based on equation (3) the state of the connection *FC*→*BAT* is given by:

$$F_{FC\rightarrow BAT}^{Pow}(t) = \varepsilon_{FC}(t) \cdot P_{FC}^{Pow} = \varepsilon_{FC}(t) \cdot P_{LD}^{Pow} \quad (13)$$

Equation (13) means that the *FC* provides the exact amount of power required by the *LD*.

2.4. Pinch Analysis

Apparently, different PMS may result from combinations of logical operators or values imposed on the *Up* and *Lo* operating limits of equation (7). Each limit represents a practical system operating goal hence it is necessary to select the PMS that allows the system to operate without violating any of the limits. For example, it may be desirable to avoid using the *DSL* hence the PMS must be selected that prohibits the state of charge of the battery ($SOAcc^{BAT}$) to drop below a *Lo* limit. It may also be desirable to avoid overcharging the battery hence the selected PMS must be the one that prohibits the $SOAcc^{BAT}$ to climb above an *Up* limit. The association of similar limits with the system operating goals has been discussed extensively in Giaouris et al. (2013, 2015).

The concept of the Pinch analysis (Giaouris et al. 2015) may be used to enable the system operation without violating the corresponding limits. Assume a set *Q* of diverse PMS that can be used in a hybrid system within each interval *k*, i.e. $Q=\{PMS_{i,k}\}$, $i \in \mathbb{N}$. For any $PMS_{i,k} \in Q$ the plot of $SOAcc^{l}$ vs. time for a range of initial conditions gives the system's PGCC (Figure 2a). A major requirement in hybrid systems is to avoid the use of outsourced energy supply (*OES*) when $SOAcc^{l}$ for any PMS drops below a limit *Lo* (e.g., due to insufficient energy in the accumulator, an external source is

306 required to satisfy the load demand). As shown in Figure 2a even for the same PMS and under the
307 same weather and load demand profiles the PGCC will depend on the value of $SOAcc^l$ at t_0 and will
308 inevitably result in different *OES*. In order to better describe the system state, term $SOAcc^l$ also
309 receives a superscript indicating the shifted level. Finding the PGCC that corresponds to the
310 maximum *OES* (called *MOES*) ensures that by covering this energy from RES the system will
311 operate without the use of an outsourced energy supply. Selecting and shifting the PGCC that
312 corresponds to the *MOES* until it pinches the *Lo* limit at $t_{\min}$ (i.e. $SOAcc^l(t_{\min})$) indicates the amount
313 of energy required to be available in the accumulator at t_0 (i.e. amount of $SOAcc_2^l(t_0)$) to avoid the
314 use of non-RES (Figure 2b).

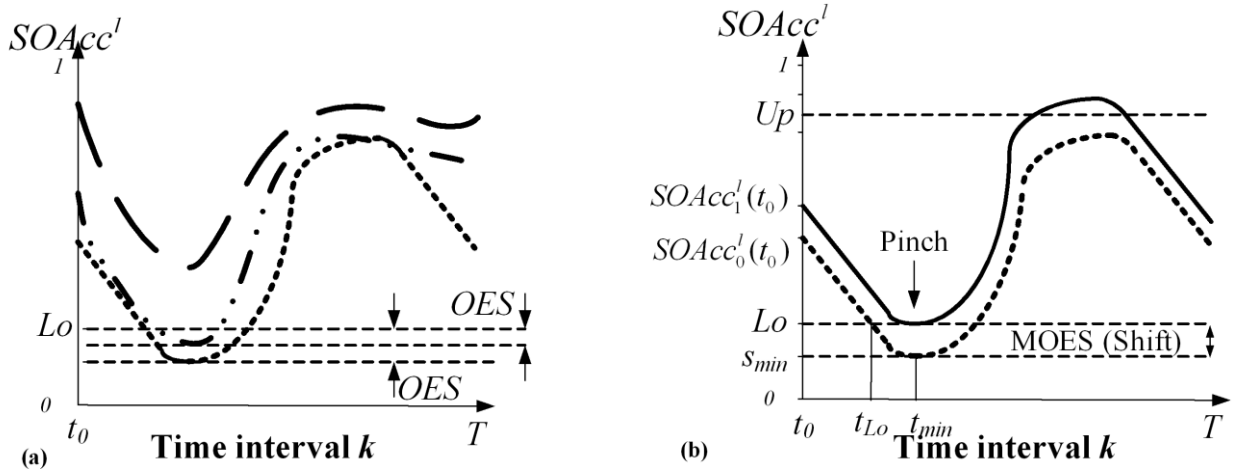

315

316 **Figure 2:** a) PGCCs for various initial values of $SOAcc^l$, b) Shift and Pinch of PGCC.

317 The concepts of the PGCC shift and the Pinch point are clearly very convenient if they are used
318 within a model predictive control framework (Giaouris et al., 2015). Assuming that a time interval
319 with duration 24 hours sufficiently describe the system behaviour, a prediction horizon of length 2
320 intervals (time intervals k and k+1) can be assumed for the satisfaction of the system goals for a
321 selected PMS. A suitable control time horizon of size one time interval (interval k) is considered.
322 The control actions involve those decisions about the sequence of equipment utilisation and
323 operating patterns in the form of a PMS that satisfy the desired goals. In this context, it is possible

to implement a *stored energy targeting step* which essentially involves the identification of the $SOAcc_1^I(t_0)$ in the prediction horizon ending at *k*+1 interval based on the procedure described above and depicted in Figure 2b. Then in a *target matching step* it is possible to compare all the available PMS in the control horizon *k* and to identify the one that best matches the target for stored energy $SOAcc_1^I(t_0)$ identified during the prediction horizon. This will allow the system to have sufficient energy at t_0 in the time interval *k*+1 so that it will avoid the use of outsourced electricity, assuming that the weather forecast at this interval is sufficiently accurate.

Although the Pinch concept is clearly useful, the utilization of pre-determined PMS includes some challenges. As shown in Figure 2b it is likely that the shift in the PGCC violates an *Up* or other limit which corresponds to an important operating goal (e.g. in case of violation turn off the *PV* to avoid overcharging the battery), as noted previously in this section. The *Up* limit clearly reveals an opportunity to exploit an additional Pinch point (by shifting the PGCC downwards) which will indicate the amount of energy (expressed as *SOAcc*) that needs to be used internally by the system in order to avoid tuning off the PVs and hence wasting renewable energy. However, if there is no available PMS that can simultaneously satisfy both limits the only way out is to prioritize the operating goals hence satisfying the one goal at the expense of the others (e.g., avoidance of outsourced electricity from non-RES at the expense of battery overcharging). An additional challenge from using pre-determined PMS is that the desired $SOAcc_1^I(t_0)$ at interval *k*+1 may not be exactly matched at the end of interval *k* (*T*). The selection of a PMS that results in $SOAcc^I(T) > SOAcc_1^I(t_0)$ means that more than the necessary renewable energy is saved during interval *k* for the subsequent time interval *k*+1, which may have detrimental effects on the system ability to satisfy the *LD* or on other important operating goals at interval *k*. Obviously, the case of $SOAcc^I(T) < SOAcc_1^I(t_0)$ is ruled out because it does not guarantee the satisfaction of the *Lo* limit

347 at interval k+1. Clearly, the concept of a pool of pre-determined PMS requires the evaluation of a
348 very large number of PMS in order to ensure that no operating constraint is violated and that the
349 energy targets identified from the PGCC may be fully matched and exploited. Although this may be
350 theoretically plausible, it becomes practically challenging because the sub-system interactions
351 represented within a PMS become increasingly complex as more sub-systems are added.
352 Furthermore, the RES behaviour always remains unpredictable hence there is no guarantee that the
353 energy recovery targets identified by Pinch analysis will be matched by the available PMS.

354 **3. PGCC Shaping**

355 **3.1 Basic steps**

356 The proposed approach exploits the PGCC concept together with the previously presented structural
357 and temporal models to develop a new method which does not rely on pre-determined PMS. Instead,
358 the PMS that supports the operation of the hybrid system is determined in the course of the system
359 operation by appropriately shaping a new system PGCC so that multiple operating goals and
360 constraints are satisfied within the same interval. The system PMS is based on a general temporal
361 model which follows a different rationale compared to depending entirely on the state of charge of
362 the accumulator, as in equation (7). This is approached through a procedure consisted of two
363 successive steps which can be used iteratively within multiple time intervals to adapt the system
364 operation under variable environmental conditions:

365 - The *stored energy targeting* step involves the identification and shifting of the PGCC during
366 the prediction horizon of length one time interval to identify the operational profile of a
367 desired accumulator within this horizon in order to avoid the violation of constraints and
368 satisfy the system operating goals.
369 - The *target matching* step requires the exact matching of the profile of the shifted PGCC in
370 the control horizon through the automatic formulation of a PMS that exploits converters and

accumulators at appropriate time instances. If more than one converters can be activated to achieve the target, then it is possible to impose more conditions through the variables ε^{Gen}.

The proposed approach assumes a system operating within an overall time span H, divided into equal time intervals (usually 24 hours). Each interval is divided into subintervals $[t_0, T]$ of duration $\Delta T=T-t_0$ hence for the k^{th} interval $t_0=(k-1)\Delta T$ and $T=k\Delta T$. Subintervals correspond to the time interval used for system simulation purposes. Prediction and control horizons coincide as the dynamics are instantaneous and the effect of the control actions become immediately observed in the system states. The next sections analyse the implementation of the above two steps considering different operating goals.

3.2 Avoidance of outsourced electricity supply –*Lo* type limit

Figures 3a and 3b illustrate the two steps through a case that assumes a limit of *Lo* type. The operating goal is to avoid obtaining a PGCC that violates the *Lo* limit as it signifies a need for outsourced electricity supply (*OES*), assuming that an accumulator such as a battery is used. It is assumed that the initial value of the $SOAcc^l$ is at $SOAcc_0^l(t_0)$. The *stored energy targeting* step proposes the shifted PGCC (continuous curve in Figure 2a) which initially indicates the required state of charge of the desired accumulator at t_0 ($SOAcc_1^l(t_0)$) in order to avoid the use of *OES*. This means that by operating the system starting from $SOAcc_1^l(t_0)$ instead of $SOAcc_0^l(t_0)$ the violation of the *Lo* limit will be avoided. However, since the $SOAcc_1^l(t_0)$ is not available at t_0 it is possible to start the operation from $SOAcc_0^l(t_0)$ and activate a converter which will increase the energy or material level of the accumulator only until the shifted PGCC is reached. In Figure 3b, the new PGCC of the system will consist of the arrow (activation of a converter) and the dotted-continuous line which coincides with the previously shifted PGCC after t_1. This new PGCC is the one that should be matched in the *target matching* step through an appropriate PMS.

In Figure 3a the original PGCC (dashed line) and the shifted PGCC (continuous line) follow the same PMS (determined in a previous interval) with the only difference that they start from a different $SOAcc^l$ at t_0. As a result, the only change required to determine a new PMS in Figure 3b in order to be able to follow the shifted PGCC is the activation of a converter (in this particular case of a *Lo* limit). The operation of the converter could last for a minimum $\Delta t=t_1-t_0$ if the converter can produce the power or material required to fill the accumulator within this Δt. If the converter has a lower capacity then the charging of the accumulator will last longer.

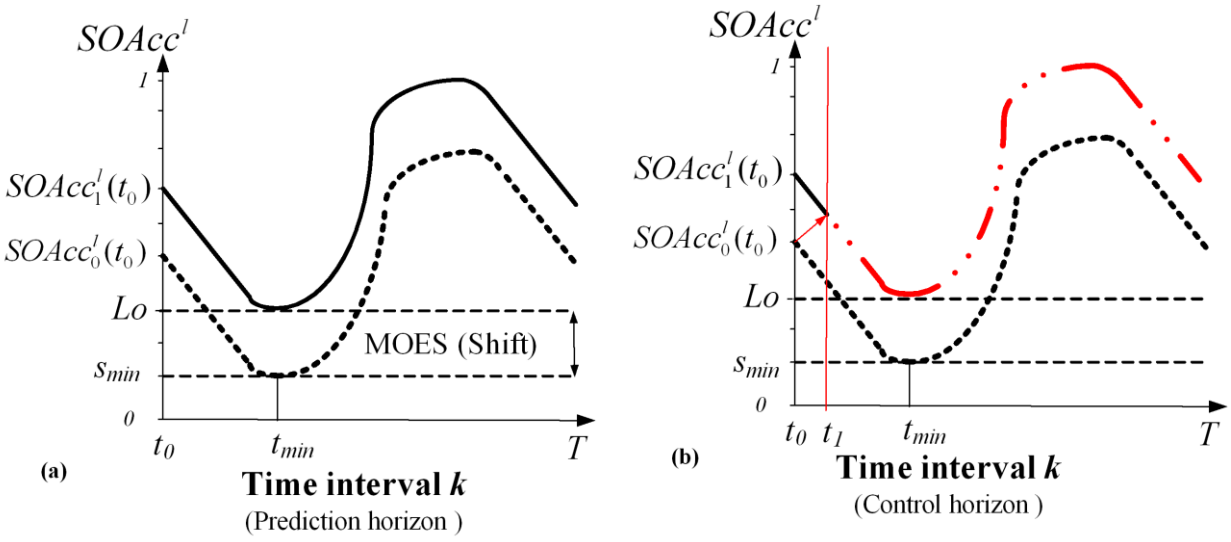

Figure 3: a) Original (dashed line) and shifted (continuous line) system PGCC, b) Activation of a converter (red arrow) to follow the shifted PGCC (dashed-double dotted line is desired part of the shifted PGCC).

At this point it is necessary to develop the model that will become the system's PMS. Shifting the PGCC up effectively means that the system is forced to start at $SOAcc_1^l(t_0)$ in order to ensure that $SOAcc_1^l(t_{min}) = Lo$. The point s_{min} can be calculated by $s_{min} = \min_{t\in[t_0,T]}\left(SOAcc_0^l(t)\right)$ hence:

$$SOAcc_1^l(t_0) = Lo - s_{min} + SOAcc_0^l(t_0) \quad (14)$$

The key idea is that if energy is provided by an appropriate converter to the system that starts from $SOAcc_0^l(t_0)$ such that $SOAcc_0^l(t_1) = SOAcc_1^l(t_1)$, then without further use of this converter (or

411 outsourced energy supply) the *Lo* limit will not be violated. The appropriate amount of energy *E*
412 (kWh) that must be provided by the converter *i* is calculated by:

413 $$E_i = C_l \cdot (Lo - s_{\min}) \tag{15}$$

414 Hence, the variable $\rho_i^{SOAcc^l}(t)$ (the condition in order to initiate the required converter and provide
415 the necessary flow) defined in equation (7) is equal to:

416 $$\rho_i^{SOAcc^l}(t) = \begin{cases} 1, & t = t_0 \\ 0, & \text{Otherwise} \end{cases} \tag{16}$$

417 Note that the use of equation (16) is independent of the state of charge of the accumulator. As an
418 example of the aforementioned analysis, assume that the accumulator *l* is the *BAT*. The *FC* is a
419 converter that may be used in this case in order to develop the overall PMS. By injecting power
420 from the *FC* to the system it is possible to reach the desired $SOAcc_1^l(t_1)$ hence avoiding the violation
421 of the *Lo* limit and the utilization of the *DSL*. Instead of using equation (8) the system PMS around
422 the *FC* and associated calculations will be performed as follows:

$$\begin{aligned}
&\rho^{SOAcc^{BAT},FC}(t) = \begin{cases} 1, & t = 1 \\ 0, & \text{Otherwise} \end{cases} \\
&F_{FC\to BAT}^{Pow}(t) = \varepsilon_{FC}(t) \cdot P_{FC}^{Pow} \\
&E_{FC} = C_{BAT} \cdot (Lo - s_{\min}) \\
&\rho_{FC}^{SOAcc^{FT}}(t) = SOAcc^{FT}(t) > Lo_{FC}^{SOAcc^{FT}}(t) \\
&\rho_{FC}^{SOAcc^{WT}}(t) = SOAcc^{WT}(t) < Up_{FC}^{SOAcc^{WT}}(t) \\
&\varepsilon_{DSL}(t-1) = 0
\end{aligned} \tag{17}$$

424 The full set of equations that define a generic structure of the PMS around all the other accumulators
425 and converters is given in the Appendix for this and the subsequently investigated cases. Notice that
426 the state of the connection $F_{FC\to BAT}^{Pow}(t)$ is different to that of equation (13), which depends on the
427 extent of shift that is required. Note that if the power (kW) required from the *FC* is higher than the
428 maximum power that it can provide (P_{FC}^{Max}), then the induced power will be P_{FC}^{Max} but the injection
429 will last for $\left\lceil \frac{E_{FC}}{P_{FC}^{Max}} \right\rceil$ hours so that $SOAcc_0^{BAT}\left(\left\lceil \frac{E_{FC}}{P_{FC}^{Max}} \right\rceil\right) = SOAcc_1^{BAT}\left(\left\lceil \frac{E_{FC}}{P_{FC}^{Max}} \right\rceil\right)$. Without loss of
430 generality and in order to facilitate the elaboration of the proposed concepts it will be assumed that

within 1 hour the *FC* can provide all the demanded energy. Hence in equations (17) P_{FC}^{Pow} equals to E_{FC} divided by 1 hour. Note that the proposed approach also supports different cases where the FC may operate as long as required.

3.3Avoidance of overcharging and outsourced electricity supply-*Lo* and *Up* type limits

The *Up* type limit may correspond to conditions where a converter must be deactivated for reasons of safety or protection of other equipment. For example, it may correspond to the undesired but necessary deactivation of the *PV* to protect the *BAT* from overcharging at the expense of wasting renewable energy in conditions of high solar radiation. The violation of an *Up* limit is addressed through the PGCC approach by a downward shift until the PGCC pinches the *Up* limit (Giaouris et al., 2015). When the two limits co-exist, the upward (in a *Lo* limit) or downward (in an *Up* limit) shift in the PGCC may result in the satisfaction of one of them but it may also result in violation of the other. Based on the proposed method, this situation may be avoided as follows:

- By performing two successive, separate shifts in the *stored energy targeting* step; first in the original PGCC (Figure 4a) and then in the shifted PGCC (Figure 4b) hence finding the pinch points in both limits.
- By matching the two separate profiles of the PGCC through the initiation of the necessary converters (Figure 5a and b); these actions will form the new PMS.

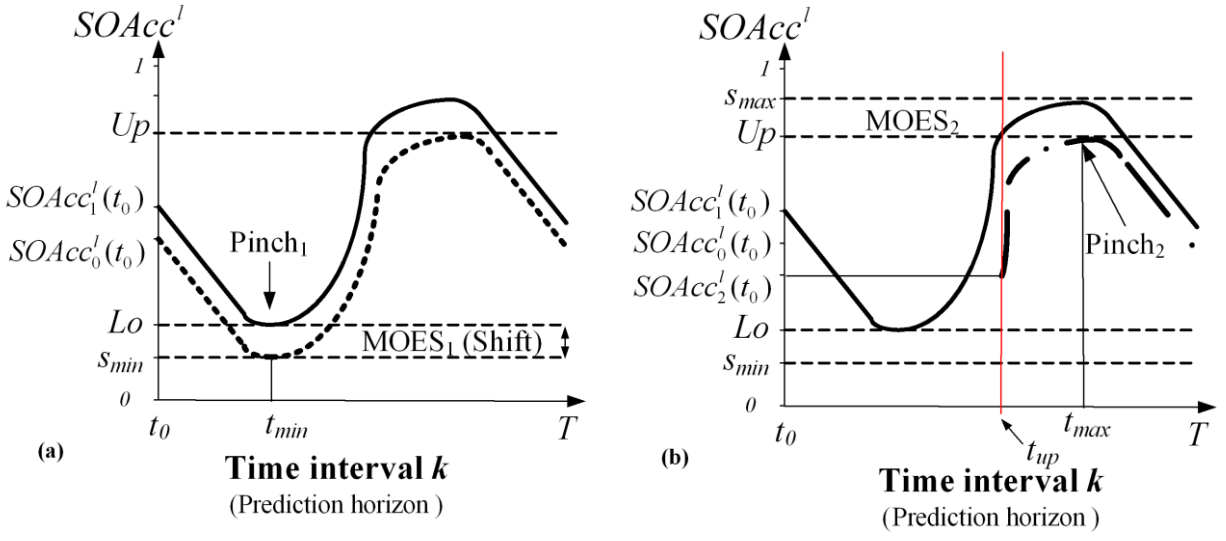

Figure 4: a) The first shift of the PGCC starting from $SOAcc_0^l(t_0)$ serves to identify Pinch$_1$ and avoid the *Lo* limit (the dashed line is the original PGCC and the continuous is the shifted PGCC), b) The second shift of the PGCC starting from $SOAcc_1^l(t_0)$ after instant t_{up} serves to identify Pinch$_2$ and avoid the *Up* limit (the dashed-dotted line is the shifted PGCC in this case).

Figure 4 describes the actions in the *stored energy targeting* step. In Figure 4a the shift is implemented as described in the previous section to find Pinch$_1$ at the *Lo* limit, disregarding the violation of the *Up* limit. Figure 4b serves to find Pinch$_2$. The instant t_{up} is identified at the point where the shifted PGCC (continuous black line) violates for the first time the *Up* limit and then only the part of the shifted PGCC after t_{up} is shifted down in order to identify Pinch$_2$.

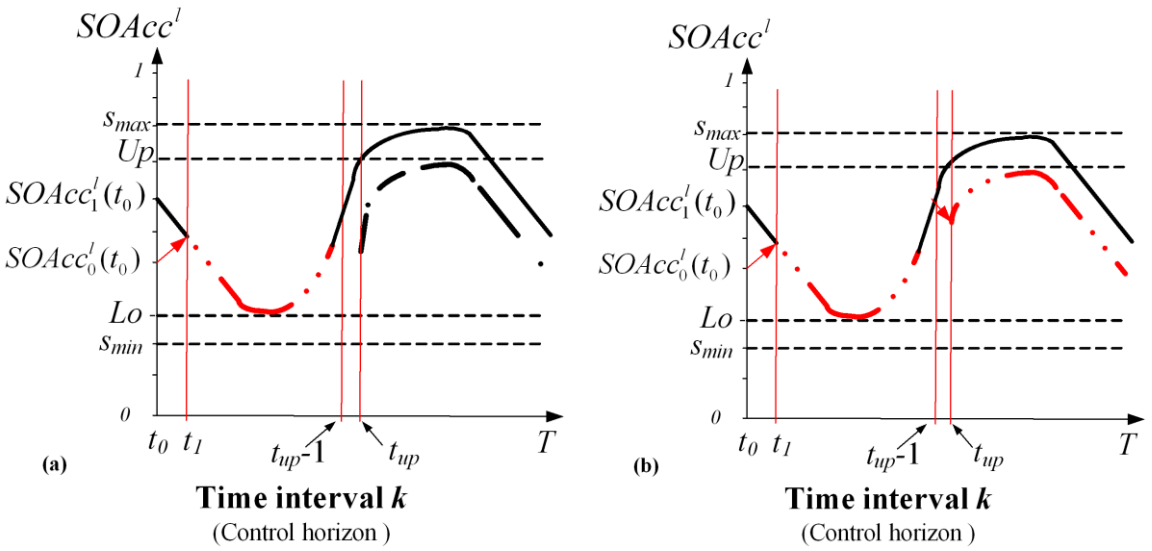

Figure 5: a) A converter is activated between t_0 and t_1 to charge the accumulator until the shifted PGCC starting from $SOAcc_1^l(t_0)$ and the shifted PGCC is followed until t_{up}-1 (the arrow and dashed-double dotted line are the desired parts of the PGCC), b) a converter is activated between t_{up}-1 and t_{up} until the shifted PGCC (dashed-dotted line) which is then followed (the new arrow and the dashed-double dotted line are the desired parts of the PGCC).

Figure 5 describes the actions in the *target matching* step. Figure 5a indicates the procedure that is described in the previous section regarding the new PMS. A converter is initiated from t_0 until t_1

which will increase the energy or material level of the accumulator until the shifted PGCC is reached. This PGCC will indicate the instant t_{up}, when the accumulator exceeds the *Up* limit. The PMS that represents the shifted PGCC will be followed until instant t_{up}-1 which is selected as one subinterval (or as many as required) away from $t_{up.}$ in order to initiate a control action which will avoid the violation of the *Up* limit. Figure 5b indicates the procedure after t_{up}-1. At t_{up}-1 a new converter will be activated (arrow between t_{up}-1 and t_{up}) which will discharge the accumulator enough (i.e., reduce the $SOAcc^{l}$) so that the curve resulting from the second shift ($Pinch_2$ at the *Up* limit of Figure 4b) may be followed in order to avoid violation of the *Up* limit. Note here that the activation of the converter that will discharge the corresponding accumulator may be implemented anytime between t_{min} and t_{up}-1. The overall PGCC will have a completely new shape as it will be a composite of the two arrows and the two red lines (dashed line with double dots until t_{up}-1 and dashed line with single dot after that).

The development of a model for the representation of the composite PGCC of Figure 5b through a PMS is based on equations (15) and (16). Assuming that the converter utilized in this case is the *EL* its activation will be based on the following rule:

$$\rho_{EL}^{SOAcc^{BAT}}(t) = \begin{cases} 1, & t = t_{up} - 1 \\ 0, & \text{otherwise} \end{cases}$$

$$E_{EL} = C_{BAT} \cdot (s_{\max} - Up)$$

$$\rho_{EL}^{SOAcc^{WT}}(t) = SOAcc^{WT}(t) > Lo_{EL \to BF}^{SOAcc^{WT}}(t)$$

$$\rho_{EL}^{SOAcc^{BF}}(t) = SOAcc^{BF}(t) < Up_{EL \to BF}^{SOAcc^{BF}}(t)$$

$$\varepsilon_{EL}^{Avl}(t) = \rho_{EL \to BF}^{SOAcc^{BAT}}(t) \wedge \rho_{EL \to BF}^{SOAcc^{WT}}(t) \quad (18)$$

$$\varepsilon_{EL}^{Req}(t) = \rho_{EL \to BF}^{SOAcc^{BF}}(t)$$

$$\varepsilon_{EL}^{Gen}(t) = 1$$

$$\varepsilon_{EL}(t) = \varepsilon_{EL \to BF}^{Avl}(t) \wedge \varepsilon_{EL \to BF}^{Req}(t) \wedge \varepsilon_{EL \to BF}^{Gen}(t)$$

$$F_{BAT \to EL}^{Pow}(t) = \varepsilon_{EL}(t) \cdot P_{EL}^{Pow}$$

where $Up = SOAcc_2^{BAT}(t_{\max})$ and $s_{\max} = \max_{t \in [t_0, T]} \left(SOAcc_0^{BAT}(t) \right)$.

3.4 Returning to the initial state of charge- *Lo, Up* and *End* type limits

A desired condition in such systems may be to achieve a full cycle in the charging-discharging process of an accumulator in the end of a time interval. The concept is illustrated in Figure 6. This means that in the end of the current interval the state of charge of the accumulator (*SOAcc*) should be the same as in the beginning of the interval hence $SOAcc_2^l(t_0) = SOAcc_2^l(T-1)$. Note that the interval end is defined as the instant when the *SOAcc* is last checked, hence the *T*-1. Such an example is the case of a *BAT* where a 24 hour interval is assumed with a subinterval of one hour and it is important to achieve $SOAcc_2^{BAT}(00:00) = SOAcc_2^{BAT}(23:00)$ (i.e., *T*=23:00 h). If $SOAcc_2^{BAT}(00:00) > SOAcc_2^{BAT}(23:00)$ then the *BAT* will end up discharged and it may result in the future activation of the *DSL*. If $SOAcc_2^{BAT}(00:00) < SOAcc_2^{BAT}(23:00)$ then the *BAT* contains excess energy that may be transformed and stored as hydrogen. This is achieved by directly activating a converter such as the *FC* at instant *T*-1 (i.e. at *t*=22:00 h). The activation takes place at the end of the control horizon. In case that it is necessary to discharge the *BAT* and produce hydrogen through the operation of the *EL*.

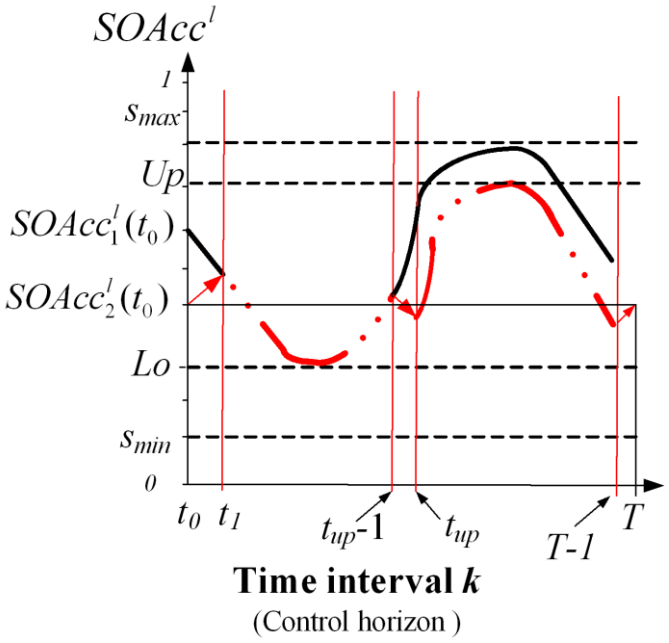

Figure 6: An appropriate converter is activated so that in the end of this interval state of charge of

501 the accumulator (*SOAcc*) becomes the same as in the beginning of the interval.

502

503 To develop a model for the PMS, the energy that must be provided in Figure 6 (or removed in a

504 similar case) should be equal to $|\Delta S| \cdot C_{BAT}$, where $\Delta S = SOAcc_2^I(t_0) - SOAcc_2^I(T-1)$. Considering

505 that the *FC* will be used in a case of charging and the *EL* in the case of discharging the overall

506 equations will take the following form:

507
$$\rho_{FC}^{SOAcc^{BAT}}(t) = \begin{cases} 1, & [t = t_0] \vee [t = T\text{-}1 \wedge \Delta S < 0] \\ 0, & Otherwise \end{cases} \quad (19)$$

508
$$\rho_{EL}^{SOAcc^{BAT}}(t) = \begin{cases} 1, & [t = t_{up} - 1] \vee [t = T\text{-}1 \wedge \Delta S > 0] \\ 0, & Otherwise \end{cases} \quad (20)$$

509
$$E_{FC} = \begin{cases} C_{BAT} \cdot (Lo - s_{\min}) & [t = t_0] \wedge [Lo > s_{\min}] \\ |\Delta S| \cdot C_{BAT} & [t = T - 1] \wedge [\Delta S < 0] \\ 0 & Otherwise \end{cases} \quad (21)$$

510
$$E_{EL} = \begin{cases} C_{BAT} \cdot (s_{\max} - Up) & [t = t_{up} - 1] \wedge [Up < s_{\max}] \\ |\Delta S| \cdot C_{BAT} & [t = T - 1] \wedge [\Delta S < 0] \\ 0 & Otherwise \end{cases} \quad (22)$$

511
$$F_{BAT \to EL}^{Pow}(t) = \varepsilon_{EL}(t) \cdot P_{EL}^{Pow}$$
$$F_{FC \to BAT}^{Pow}(t) = \varepsilon_{FC}(t) \cdot P_{FC}^{Pow} \quad (23)$$

512 **4. Implementation**

513 The proposed developments will be illustrated in case studies where the system PMS is developed

514 using the *FC* and the *EL* as the converters which are initiated to match the desired PGCC. The *DSL*

515 is also used as a back-up option. The first case study illustrates important features of the method

516 within a 24 hours interval. The second case study considers two cases. Firstly, yearly historical

517 weather data are employed to emulate an accurate (ideal) forecast and demonstrate the

implementation of the proposed approach. In the second case random variations obtained from a normal distribution are imposed on the historical weather data, to emulate the weather unpredictability and investigate the performance of the proposed approach under realistic operating conditions (i.e., predicted and actual weather conditions do not match). The system is simulated for a 24 h time interval *k* within a yearly horizon, using averaged hourly weather data. It is therefore assumed that t_0=00:00 and T=23:00 at every interval. The *LD* is assumed constant at 1.5kW, the employed RES is the PV and the BAT capacity is C_{BAT}=144kW. Note that the method may also be implemented for a variable *LD* demand and other *RES*. Specific technical system characteristics are obtained from Giaouris et al. (2013). It is assumed that the system is activated in January 1st with the following initial state status: $SOAcc_0^{BAT}(00:00)=0.25$, $SOAcc_0^{FT}(00:00)=0.8$, $SOAcc_0^{BF}(00:00)=0.5$, $SOAcc_0^{WT}(00:00)=0.7$, $\varepsilon_{PV}(00:00)=1$, $\varepsilon_i(00:00)=1\ \forall i \in Rs^{Conv}$, excluding the connections between *PV* and *BAT* as well as *BAT* and *LD*. The *Lo* limit is set at $SOAcc^{BAT}$=0.2 (i.e., *Lo*=0.2), the *Up* limit at $SOAcc^{BAT}$=0.8 (i.e., *Up*=0.8) and the *End* limit condition is that $SOAcc_0^{l}(00:00)=SOAcc_0^{l}(23:00)$

5. Results and discussion

5.1 Illustration of the proposed approach

The daily power delivered by the PV is shown in Figure 7a whereas the PGCC for the initial conditions is shown in Figure 7b (blue solid line). The minimum value of the system PGCC is s_{min} =0.1581 and the required shift is *Lo*-s_{min} =0.0419. From equation (14) the shifted PGCC (dots of Figure 7b) will be at $SOAcc_1^{BAT}(00:00)=0.2919$ and as expected it presents a pinch at the value of 0.2. The minimum outsourced electricity supply required by the system is given by the shifted curve at 0.0491. This implies that the power required by the *FC* at t_0=00:00 is P_{FC}^{Pow} =0.0491·144=7.07 kW

based on equation (15). Figure 7b shows the new PGCC (red solid line) response when the desired amount of power is provided by the *FC* for 1 hour.

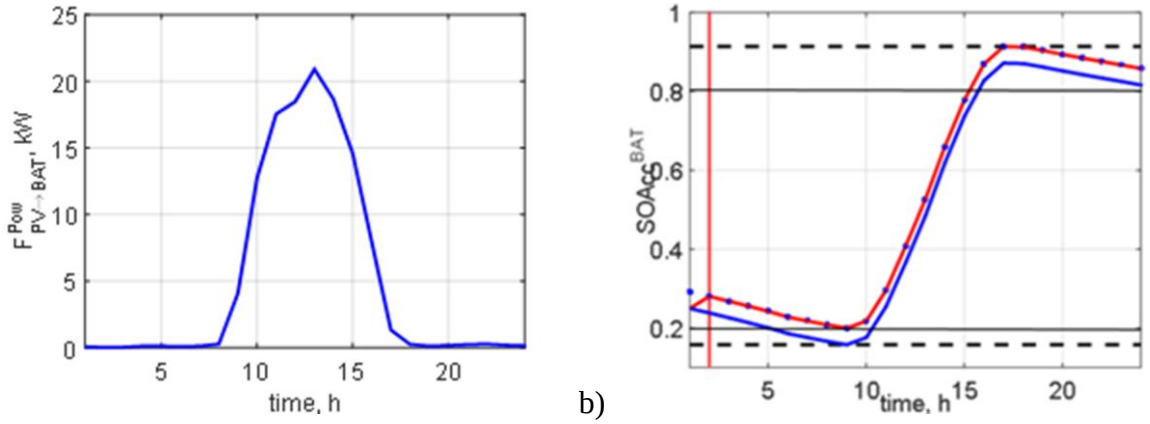

a) b)

Figure 7: a) Daily power profile delivered from the PV, b) The system PGCC (blue solid line), the system shifted PGCC (dots) and the new PGCC after initiation of the FC to avoid the Lo limit (red solid line). The intensely dashed lines indicate the s_{min} and s_{max}.

The *Up* limit is addressed by first noticing that the shifted PGCC (which aimed at avoiding the Lo limit in Figure 7b) has s_{max}=0.9138, i.e. the required shift is *Up*-s_{max}=0.1138. Based on the availability of hourly weather data that is assumed here, the first time where a sample is higher than this limit is at t_{up}=16:00. Hence, the amount of energy that must be consumed by the *EL* is P_{EL}^{Pow} =0.1138×144=16.38 kW and it will be activated at t_{up-1}=15:00. Figure 8 shows the response of the system when it violates the *Up* limit (blue line) and with the correction when the *EL* is activated at 15:00 (red line).

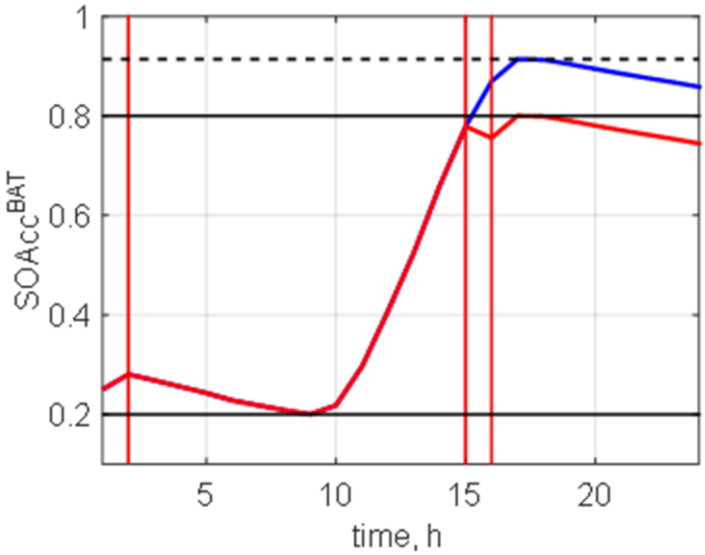

554

555 **Figure 8:** The new PGCC after initiation of the *FC* to avoid the *Lo* limit (red line until 15:00 and
556 blue line after that), the PGCC of the initiated EL between 15:00 and 16:00 and the new downward
557 shift in the PGCC after 16:00 (red line after 16:00).

558

559 The last condition associated with the *End* type limit, i.e. that $\Delta S = SOAcc^{l}(t_0) - SOAcc^{l}(T-1) = 0$,
560 is investigated using the *EL* in this case to produce hydrogen. Figure 9 shows that the last value of
561 the PGCC one time sample before the end of the time interval at T-1=22:00 is $SOAcc^{BAT}(23:00)$
562 =0.7443. Hence ΔS=0.7443-0.25=0.4943 and therefore at t=23:00 the *EL* must be activated in order
563 to remove 0.4943×144=71.18kW and produce the corresponding hydrogen. If more power is
564 required than the maximum that the *EL* can consume (in this case of 71kWh) then the *EL* can be
565 activated for a longer duration as long as the consumed energy forces ΔS=0. Figure 9 shows that
566 indeed by activating the EL at t=21:00 for 2 hours we have that
567 $SOAcc^{BAT}(00:00) = SOAcc^{BAT}(24:00)$ which proves that the PGCC can be completely shaped
568 according to practically any design restriction. The changes in the system operation are implemented
569 through the PMS that are developed in the course and as a result of the PGCC shaping.

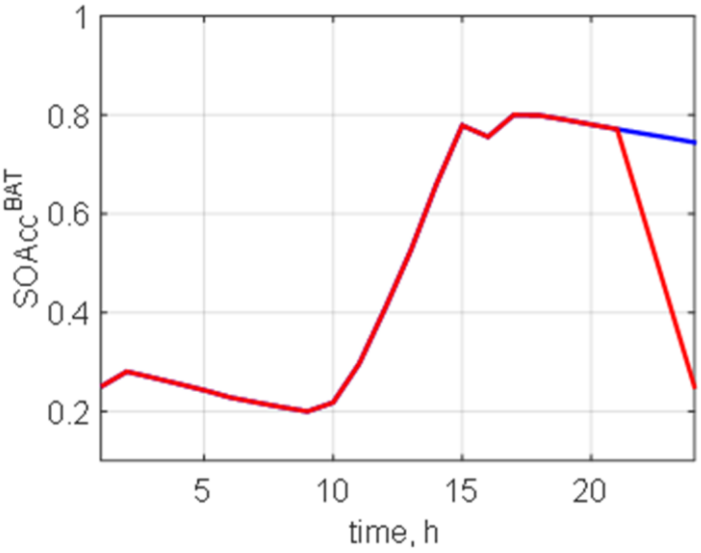

Figure 9: Discharge of the BAT after 21:00 using the EL to meet the *End* type limit. The blue trace is the PGCC that resulted after the 2nd shift and the red trace is the PGCC that includes all three shifts.

5.2 Year-round operation

Ideal weather forecasting

To further investigate the proposed approach, the yearly operation of the system is investigated under again ideal weather forecasting. As ideal weather conditions are used, the main issue that needs to be investigated is the performance of the system for different values of the limit *Lo*, *Up* and *End*. Figure 10 shows the response of the system when the operational limits are *Lo*=0.3, *Up*=0.7 and the initial $SOAcc^{BAT}$(00:00) takes the following values 0.69, 0.6, 0.5, 0.4 and 0.31. These values were chosen as indicative for possible combinations of the three limits. We will investigate if there is a violation of the *Up*, *Lo* and *End* limits within the year and if there are combinations of limit values that result in violations.

584 a)

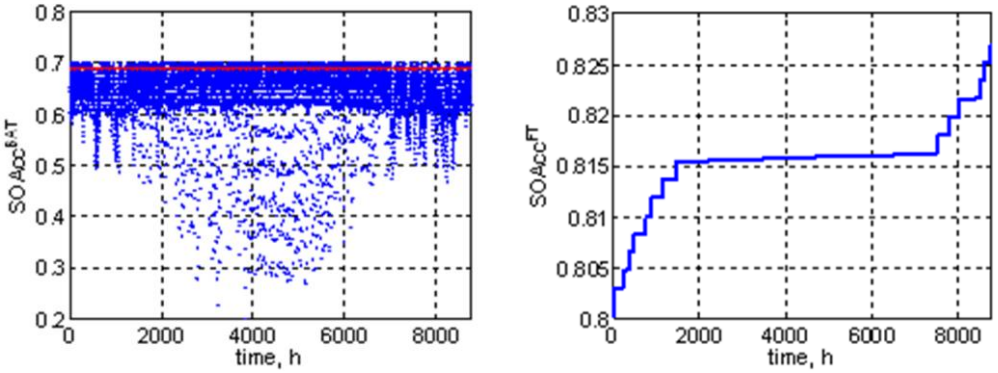

585 b)

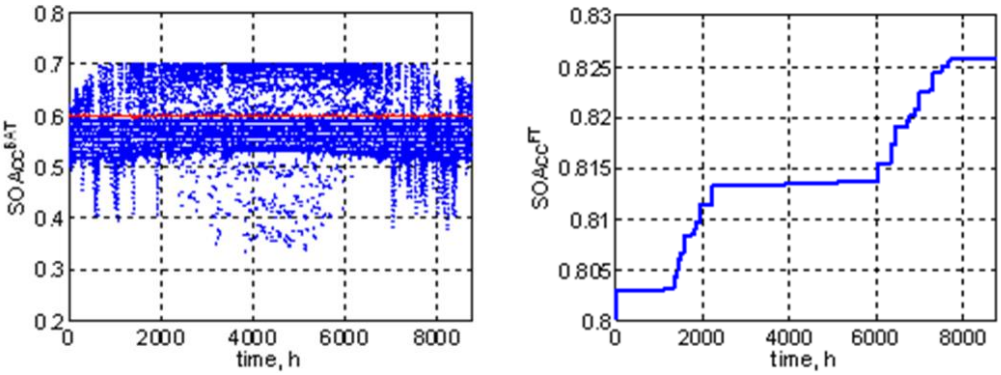

586 c)

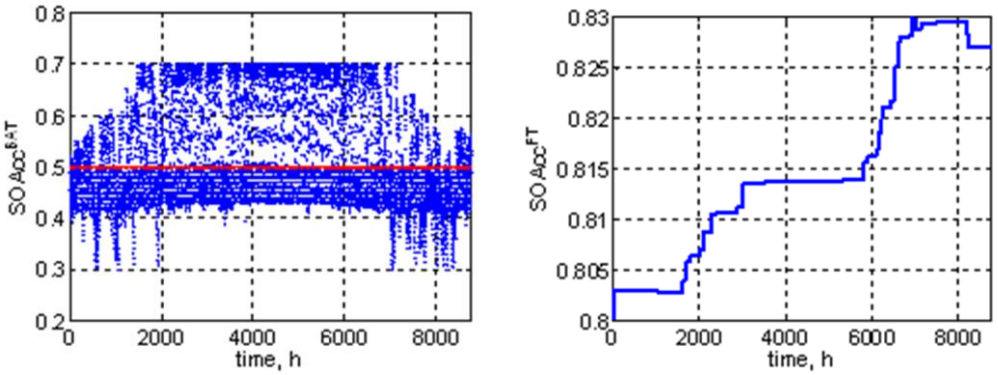

587 d)

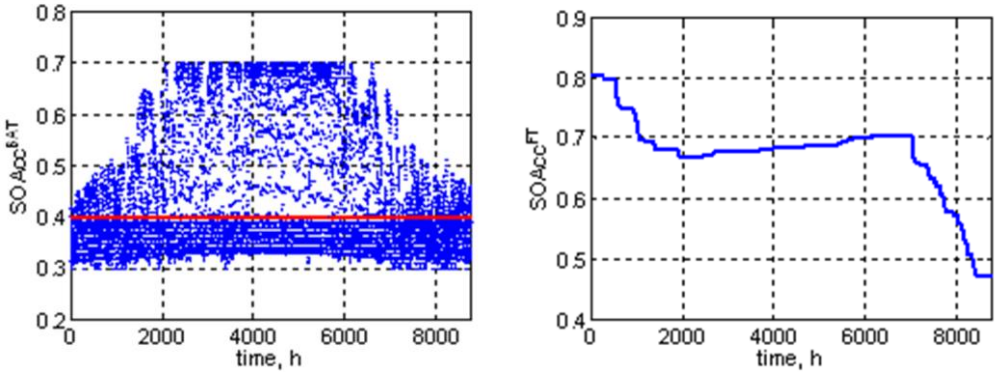

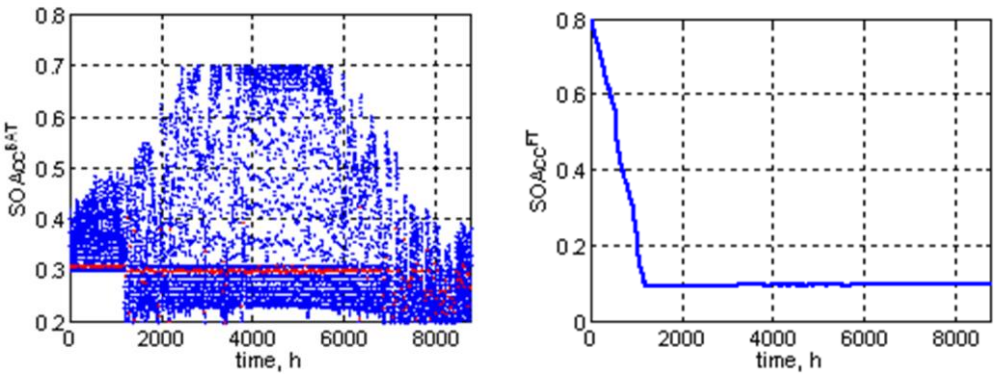

e)

Figure 10: Year round system response for ideal weather forecasting and the initial $SOAcc^{BAT}$(00:00) at a) 0.69, b) 0.6, c) 0.5, d) 0.4, e) 0.31. The left side diagrams show the responses of $SOAcc^{BAT}$ whereas the right the $SOAcc^{FT}$. The blue dots in each case correspond to the values of SOAcc sampled every 1h and the red dots the values of SOAcc sampled every 24h.

From the above figures we can see the possible responses when the three limits take different values. As expected in most cases all three limits are satisfied apart from the extreme cases (Figures 10a and 10e). A key factor here is the capacity of $SOAcc^{FT}$, as when the *End*=0.31 and *Lo*=0.3 limits are close (one type of extreme case in Figure 10e) then the *FC* has to be frequently used. This is happening because if the system starts at 00:00 close to the *Lo* limit (which was a result of the previous day *End* limit) due to the lack of power produced from the *PV* the $SOAcc^{BAT}$ will drop and hence the *FC* must be activated. Another interesting phenomenon is observed in the other extreme case (Figure 10a), where the *End* limit is very close to the *Up* limit, i.e. at the start of each day we have a charged battery. In this case the *Lo* limit is also violated but for a different reason. This is happening because during the summer the solar irradiation is high and hence as the system starts from a very high value the estimated $SOAcc^{BAT}$ becomes greater than 1. This results in an estimated power consumption by the *EL* greater than 57.6kW which is the maximum that should be removed in the zone 0.7 to 0.3 (as 0.7-0.3=0.4 and 0.4×144kW=57.6kW). Obviously, this can be altered if the maximum value of the power consumed by the *EL* is (*Up*-*Lo*) ×144kW but then the *Up* limit will be violated as not enough power is consumed. In Figures 10b,c,d where the difference between

609 the limits is higher than 0.1 the system operates within the desired constraints throughout the year
610 as the PGCC is continuously shaped according to the available renewable energy and *LD* demands.
611 ***Non-ideal weather forecasting***
612 In this section we further investigate the aforementioned methodology by introducing an error in
613 the estimation of the weather forecast and by assuming that the maximum power that we can operate
614 the *EL* is at 30kW. The error was imposed on the available yearly historical data by multiplying
615 each sample of the power produced by the PV with a random number obtained from a normal
616 distribution with mean 1 and variable variance. As a case study this variance takes the values of 0,
617 0.01, 0.05, 0.1, 0.2 and 0.5 hence the distribution used for the error in the weather predictions
618 changes at every time sample emulating different potential weather conditions. The yearlong
619 response for these cases is shown in Figure 11, and we can see that when the real and the predicted
620 weather profiles are not the same, there is a deviation between the real and the estimated PGCC and
621 obviously for high values of this variance the 3 conditions are barely met. Having said that, we need
622 to stress the fact that when the variance gets a value greater than 0.1, the distortion in the power
623 delivered by the PV is significant and probably unrealistic. Figure 12 shows the real and predicted
624 power delivered by the *PV* to the *BAT* when the variance is 0.5 for two particular days and we can
625 clearly see this difference which is unrealistic when a proper weather forecast is used for the next
626 24 h. It is therefore worth noting that the proposed method maintains the system within operating
627 limits for reasonable weather forecasting errors. For more intense variability, the proposed method
628 may still have beneficial results in its current form by actions such as considering smaller prediction
629 and control intervals where forecasts may be better.

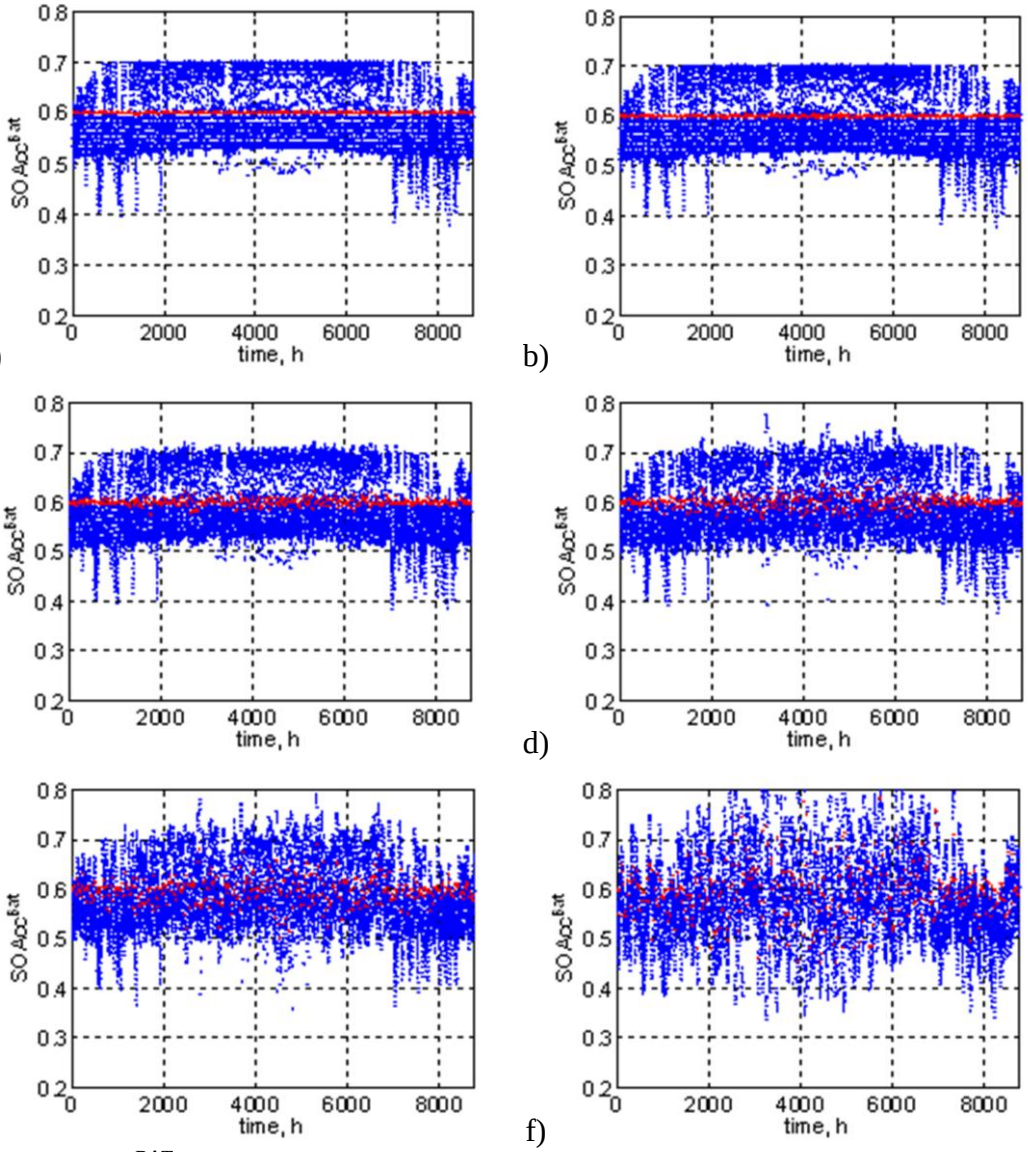

Figure 11: $SOAcc^{BAT}$ response when the variance is a) 0, b) 0.01, c) 0.05, d) 0.1, e) 0.2 and f) 0.5.

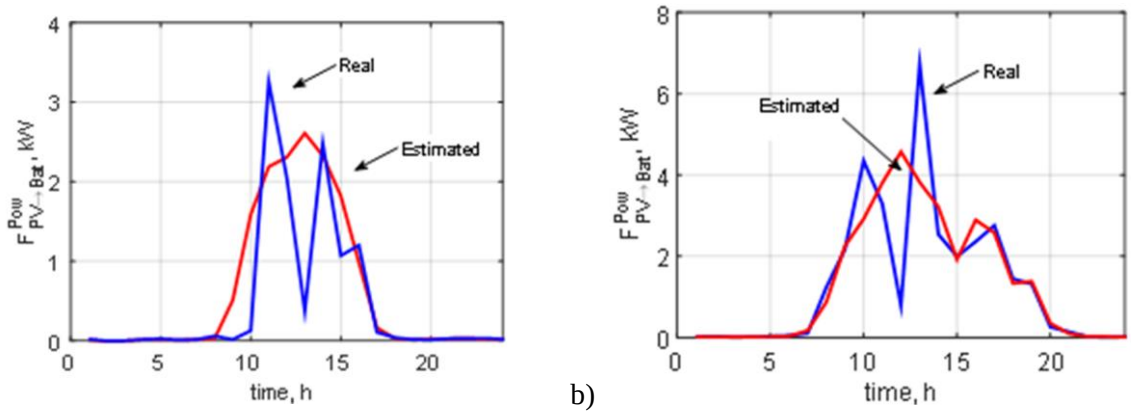

Figure 12: The power produced from the PVs during a) winter and b) summer. The blue trace is the real power produced (based on the actual weather emulated through the probability distribution

637 approach) and the red trace is the assumed (estimated) one when the response of the $SOAcc^{BAT}$ was
638 based on the weather forecast using the original historical data.

639 **6. Conclusions**

640 This work has presented a new approach which exploits the concept of PGCC to develop efficient
641 PMS in the course of operation of a hybrid microgird including energy storage. The proposed
642 approach breaks down the operation of the system into several steps within a short time interval
643 depending on the desired operating limits. The PGCC that indicates the temporal profile of the stored
644 energy is shifted independently within each step in order to identify the amount of energy that needs
645 to be utilized (produced or consumed) internally by the system and avoid the violation of important
646 operating goals. Such operating goals include the avoidance of using outsourced energy supply, of
647 overcharging particular accumulators, of wasting renewable energy at instants of high availability
648 and of allowing incomplete charge-discharge cycles of accumulators which may have detrimental
649 effects on the anticipated life term. Different parts of the shifted PGCC indicate different energy
650 recovery or utilization targets which are matched by a sequence of control actions that activate
651 desired converters for the appropriate duration in order to meet the desired operating goals.
652 The results obtained from the case studies indicate major advantages of identifying and
653 implementing the most efficient PMS in the course of the system operation than selecting a PMS
654 from a set of pre-specified ones as in Giaouris et al. (2015). The operating limits are never violated
655 and the system always satisfies the operating goals. In this respect the use of outsourced electricity
656 is completely avoided (i.e. the DSL is never activated), no renewable energy is wasted (i.e. the PV
657 are not deactivated), the BAT is never overcharged while it always completes a full charge-
658 discharge cycle from start to end of an operating time interval. Furthermore, the proposed approach
659 facilitates the protection of delicate equipment such as the FC and the EL as they are activated very
660 infrequently and with a short duration.

661 # References

662 Bandyopadhyay S (2011) Design and optimization of isolated energy systems through pinch
663 analysis. Asia-Pac J Chem Eng 6: 518-526.
664 Bizon N, Oproescu M, Raceanu M (2015) Efficient energy control strategies for a Standalone
665 Renewable/Fuel Cell Hybrid Power Source. Energ Convers Manage 90: 93-110.
666 Castañeda M, Cano A, Jurado F, Sánchez H, Fernández LM (2013) Sizing optimization, dynamic
667 modeling and energy management strategies of a stand-alone PV/ hydrogen/battery-based
668 hybrid system. Int J Hydrog Energy 38(10): 3830-3845.
669 Chauhan A, Saini RP (2014) A review on Integrated Renewable Energy System based power
670 generation for stand-alone applications: Configurations, storage options, sizing methodologies
671 and control. Renew Sust Energ Rev 38: 99-120.
672 Esfahani IJ, Lee SC, Yoo CK (2015) Extended-power pinch analysis (EPoPA) for integration of
673 renewable energy systems with battery/hydrogen storages. Renew Energy 80: 1-14.
674 Giaouris D, Papadopoulos AI, Voutetakis S, Papadopoulou S, Seferlis S (2015) A power grand
675 composite curves approach for analysis and adaptive operation of renewable energy Smart
676 Grids, Clean Techn Environ Policy 17 (5): 1171-1193.
677 Giaouris D, Papadopoulos AI, Ziogou C, Ipsakis D, Voutetakis S, Papadopoulou S, Seferlis P,
678 Stergiopoulos F, Elmasides C (2013) Performance investigation of a hybrid renewable power
679 generation and storage system using systemic power management models. Energy 61:621–635
680 Ho WS, Hashim H, Lim JS, Klemeš JJ (2013a) Combined design and load shifting for distributed
681 energy system. Clean Techn Environ Policy 15:433–444.
682 Ho WS, Khor CS, Hashim H, Macchietto S, Klemeš JJ (2013b) SAHPPA: a novel power pinch
683 analysis approach for the design of off-grid hybrid energy systems. Clean Techn Environ Policy
684 16(5): 957-970.
685 Ho WS, Mohd ZWMT, Haslenda H, Zarina AM (2014) Electric system cascade analysis (ESCA):
686 Solar PV system. Int J Elec Pow 54: 481–486.

687 Ipsakis D, Voutetakis S, Seferlis P, Stergiopoulos F, Papadopoulou S, Elmasides C (2008) The
688 effect of the hysteresis band on power management strategies in a stand-alone power system
689 energy. Energy 33: 1537–1550.
690 Ipsakis D, Voutetakis S, Seferlis P, Stergiopoulos F, Elmasides C (2009) Power management
691 strategies for a stand-alone power system using renewable energy sources and hydrogen
692 storage. Int J Hyd Energy 34 (16): 7081-7095.
693 Ziogou C, Ipsakis D, Elmasides C, Stergiopoulos F, Papadopoulou S, Seferlis P, Voutetakis S,
694 (2011) Automation infrastructure and operation control strategy in a stand-alone power system
695 based on renewable energy sources. J Power Sources 196 (22): 9488-9499.
696 Klemeš JJ (ed) (2013) Process integration handbook. Woodhead Publishing, Cambridge, UK.
697 Klemeš JJ, Varbanov PS (2013) Process Intensification and Integration: an assessment Clean Techn
698 Environ Policy 15:417–422.
699 Kuznetsov YA (2004) Elements of Applied Bifurcation Theory. Springer-Verlag, Berlin, Germany
700 Linhoff B, Flower JR (1978) Synthesis of heat exchanger networks: I. Systematic generation of
701 energy optimal networks. AIChE J 24(4): 633–642.
702 Mohammad Rozali NE, Wan Alwi SR, Klemes JJ, Yusri Hassan M (2015) A process integration
703 approach for design of hybrid power systems with energy storage. Clean Techn Environ Policy
704 17 (7): 2055-2072.
705 Mohammad Rozali NE, Wan Alwi SR, Manan ZA, Klemeš JJ Hassan MY (2014b), Cost-effective
706 load shifting for hybrid power systems using power pinch analysis. Energy Procedia 61:
707 2464-2468.
708 Mohammad Rozali NE, Wan Alwi SR, Manan ZA, Klemeš JJ, Hassan MY (2013a) Process
709 integration techniques for optimal design of hybrid power systems. Appl Therm Eng 61: 26-35.
710 Mohammad Rozali NE, Wan Alwi SR, Manan ZA, Klemeš JJ, Hassan MY (2013b) Process
711 integration of hybrid power systems with energy losses considerations. Energy 55: 38-45.

712 Mohammad Rozali NE, Wan Alwi SR, Manan ZA, Klemeš JJ, Hassan MY (2013c) Optimisation
713 of pumped-hydro storage system for hybrid power system using power pinch analysis. Chem
714 Eng Trans 35: 85-90.
715 Mohammad Rozali NE, Wan Alwi SR, Manan ZA, Klemeš JJ, Hassan MY (2014a) Optimal sizing
716 of hybrid power systems using power pinch analysis. J Clean Prod 71: 158-67.
717 Priya GSK, Bandyopadhyay S (2013) Emission constrained power system planning: a pinch
718 analysis based study of Indian electricity sector, Clean Techn Environ Policy 15:771–782
719 Sakhare A, Davari A, Feliachi A (2004) Fuzzy logic control of fuel cell for stand-alone and grid
720 connection. J Power Sources 135(1–2): 165-176.
721 Smith R (2005) Chemical Process: Design and Integration. John Wiley and Sons, New York, USA.
722 Varbanov PS, Fodor Z, Klemeš JJ (2012) Total Site targeting with process specific minimum
723 temperature difference (ΔTmin). Energy 44(1): 20-28
724 Wan Alwi SR, Rozali NEM, Manan ZA, Klemeš JJ (2012a) A process integration targeting method
725 for hybrid power systems. Energy 44: 6-10.
726 Wan Alwi SR, Rozali NEM, Manan ZA, Klemeš JJ (2012b) Design of hybrid power systems with
727 energy losses. Chem Eng Trans 29: 121-126.
728 Wan Alwi SR, Tin OS, Rozali NEM, Manan ZA, Klemeš JJ (2013) New graphical tools for process
729 changes via load shifting for hybrid power systems based on power pinch analysis. Clean Techn
730 Environ Policy 15: 459-72.
731 Zahboune H, Kadda FZ, Zouggar S, Ziani E, Klemes JJ, Varbanov PS, Zarhloule Y (2014) The new
732 electricity system cascade analysis method for optimal sizing of an autonomous hybrid PV/wind
733 energy system with battery storage, 5th International Renewable Energy Congress (IREC)
734 2014. doi: 10.1109/IREC.2014.6826962.
735

Appendix

Table A.1: Generic model of power management strategy structure.

Connection	Symbol	Equation
$PV \rightarrow BAT$	$\varepsilon_{PV}(t)$	$\bigcap_{c} \left[\varepsilon_{PV}^{c}(t) \right], c \in \{Avl, Req, Gen\}$
	$\varepsilon_{PV}^{Avl}(t)$	1
	$\varepsilon_{PV}^{Req}(t)$	$\rho_{PV}^{SOAcc^{BAT}}(t)$
	$\varepsilon_{PV}^{Gen}(t)$	1
	$\rho_{PV}^{SOAcc^{BAT}}(t)$	$SOAcc^{BAT}(t) < Up_{PV}^{SOAcc^{BAT}}(t)$
$DSL \rightarrow BAT$	$\varepsilon_{DSL}(t)$	$\bigcap_{c} \left[\varepsilon_{DSL}^{c}(t) \right], c \in \{Avl, Req, Gen\}$
	$\varepsilon_{DSL}^{Avl}(t)$	1
	$\varepsilon_{DSL}^{Req}(t)$	$\rho_{DSL}^{SOAcc^{BAT}}(t)$
	$\varepsilon_{DSL}^{Gen}(t)$	1
	$\rho_{DSL}^{SOAcc^{BAT}}(t)$	$\left[SOAcc^{BAT}(t) < Up_{DSL}^{SOAcc^{BAT}}(t) \right] \vee \left[\left[Lo_{DSL}^{SOAcc^{BAT}}(t) < SOAcc^{BAT}(t) < Up_{DSL}^{SOAcc^{BAT}}(t) \right] \wedge \left[\varepsilon_{DSL}(t-1) \right] \right]$
$CP \rightarrow FT$	$\varepsilon_{CP}(t)$	$\bigcap_{c} \left[\varepsilon_{CP}^{c}(t) \right], c \in \{Avl, Req, Gen\}$
	$\varepsilon_{CP}^{Avl}(t)$	$\rho_{CP}^{SOAcc^{BF}}(t)$
	$\varepsilon_{CP}^{Req}(t)$	$\rho_{CP}^{SOAcc^{FT}}(t)$
	$\varepsilon_{CP}^{Gen}(t)$	1
	$\rho_{CP}^{SOAcc^{BF}}(t)$	$\left[SOAcc^{BF}(t) > Lo_{CP \rightarrow FT}^{SOAcc^{BF}}(t) \right] \vee \left[\left[Lo_{CP}^{SOAcc^{BF}}(t) < SOAcc^{BF}(t) < Up_{CP}^{SOAcc^{BF}}(t) \right] \wedge \left[\varepsilon_{CP \rightarrow FT}(t-1) \right] \right]$
	$\rho_{CP}^{SOAcc^{FT}}(t)$	$SOAcc^{FT}(t) < Up_{CP}^{SOAcc^{FT}}(t)$
$FC \rightarrow BAT$	$\varepsilon_{FC}(t)$	$\bigcap_{c} \left[\varepsilon_{FC}^{c}(t) \right], c \in \{Avl, Req, Gen\}$
	$\varepsilon_{FC}^{Avl}(t)$	$\bigcap_{l} \left[\rho_{FC}^{SOAcc^{l}}(t) \right], l \in \{FT, WT\}$

	$\varepsilon_{FC}^{Gen}(t)$	1
	$\varepsilon_{FC}^{Req}(t)$	$\rho_{FC}^{SOAcc^{BAT}}(t)$
	$\rho_{FC}^{SOAcc^{FT}}(t)$	$SOAcc^{FT}(t) > Lo_{FC}^{SOAcc^{FT}}$
	$\rho_{FC}^{SOAcc^{WT}}(t)$	$SOAcc^{WT}(t) < Up_{FC}^{SOAcc^{WT}}(t)$
	$\rho_{FC}^{SOAcc^{BAT}}(t)$	$\begin{cases} 1, & [t = t_0] \vee [t = T\text{-}1 \wedge \Delta S < 0] \\ 0, & \text{Otherwise} \end{cases}$
$EL \rightarrow BF$	$\varepsilon_{EL}(t)$	$\bigcap_c \left[\varepsilon_{EL}^{c}(t)\right], c \in \{Avl, Req, Gen\}$
	$\varepsilon_{EL}^{Req}(t)$	$\rho_{EL}^{SOAcc^{BF}}(t)$
	$\varepsilon_{EL}^{Avl}(t)$	$\bigcap_l \left[\rho_{EL}^{SOAcc^{l}}(t)\right], l \in \{BAT, WT\}$
	$\varepsilon_{EL}^{Gen}(t)$	1
	$\rho_{EL}^{SOAcc^{BF}}(t)$	$SOAcc^{BF}(t) < Up_{EL}^{SOAcc^{BF}}(t)$
	$\rho_{EL}^{SOAcc^{BAT}}(t)$	$\begin{cases} 1, & \left[t = t_{up} - 1\right] \vee [t = T\text{-}1 \wedge \Delta S > 0] \\ 0, & \text{Otherwise} \end{cases}$
	$\rho_{EL}^{SOAcc^{WT}}(t)$	$SOAcc^{WT}(t) > Lo_{EL}^{SOAcc^{WT}}(t)$

738